

# Assessing the variability of hydrographic processes influencing the life cycle of the Sicilian Channel anchovy, *Engraulis encrasicolus*, by satellite imagery

JESÚS GARCÍA LAFUENTE,<sup>1,\*</sup> JUAN MIGUEL VARGAS,<sup>1</sup> FRANCISCO CRIADO,<sup>1</sup> ALBERTO GARCÍA,<sup>2</sup> JAVIER DELGADO<sup>1</sup> AND SALVATORE MAZZOLA<sup>3</sup>

<sup>1</sup>Departamento de Física Aplicada II, Universidad de Málaga, 29071 Málaga, Spain

<sup>2</sup>Centro Oceanográfico de Málaga, Instituto Español de Oceanografía, 29640 Fuengirola, Málaga, Spain

<sup>3</sup>Istituto di Ricerche sulle Risorse Marine e l'Ambiente, Consiglio Nazionale delle Ricerche, 91026 Mazara del Vallo, Italy

## ABSTRACT

Three oceanographic surveys carried out in the Sicilian Channel during the spawning season (June to July) of anchovy (*Engraulis encrasicolus*) showed a close relationship between anchovy reproductive strategy and important hydrographic structures. A time series of satellite-derived sea surface temperature images of the Sicilian Channel were analysed by means of empirical orthogonal functions and the dominant empirical modes were studied in detail. The first empirical mode captured much of the original variance and reproduced the trajectory of the Atlantic Ionian Stream (AIS), the principal hydrodynamic feature of the area. The time coefficients of modes 1 and 2 had seasonal signals which, when combined, accounted for the enhancement of the thermal front, clearly visible off Cape Passero (southernmost coast of Sicily) during summer. As the area constituted the principal nursery ground of the Sicilian Channel anchovy, the combination of the time coefficients of these modes was considered a potential indicator of the food particle concentration usually associated with oceanic fronts, which provided the energy requirements for larval growth. Mode 3 described the north/south displacements of the mean AIS trajectory, which modified the surface temperature regime of the anchovy spawning

habitat. Therefore, the time coefficients of this mode were used as a potential indicator of anchovy spawning habitat variability. The capability of time coefficients of modes 2 and 3 to modify the main pattern depicted by mode 1 were tested successfully against *in situ* oceanographic observations.

**Key words:** empirical orthogonal functions, *Engraulis encrasicolus*, hydrographic processes, sea surface temperature, Sicilian Channel, temporal variability

## INTRODUCTION

Environment has long been known to play an essential role in the recruitment success of small pelagic fish species, such as anchovies. A suite of hydrographic features, such as upwelling (either permanent or wind-induced), fronts, river plumes, and advective currents, which in turn are modulated by climatic forces, characterize the spawning habitat of these species.

In the Bay of Biscay, upwelling intensity caused by the influence of north-easterlies largely explains recruitment variability of anchovy (Borja *et al.*, 1998). However, advective losses of eggs and larvae by wind-induced currents seem to be decisive in recruitment failures of the South African anchovy, whose reproductive strategy is determined by the spawning off the Agulhas bank and the transport of eggs and larvae towards nursery grounds located 400 km downstream the Benguela current (Hutchings *et al.*, 1998).

In the Mediterranean Sea, the spawning habitat of anchovy is generally confined to shelf edges, where various kinds of enrichment processes may occur. The north-west Mediterranean anchovy population, one of the most important in the Mediterranean, is highly influenced by the shelf-slope frontal system running along the Catalanian shelf (Font *et al.*, 1988) and the fronts associated with the important discharges of the Rhône and Ebro rivers, enhancing larval survival potential (García and Palomera, 1996; Lloret *et al.*, 2004).

The Sicilian Channel anchovy whose habitat spreads over the southern coast of Sicily (Mazzola

\*Correspondence. e-mail: glafuente@ctima.uma.es

Received 18 November 2002

Revised version accepted 15 March 2004

*et al.*, 2000, 2002), developed a reproductive strategy that is coupled to the surface circulation of the Atlantic Ionian Stream (AIS) in a manner that recalls the strategy of the South African anchovy, although at a noticeably smaller spatial scale (García Lafuente *et al.*, 2002). This meandering surface current flowing towards the Ionian Sea transports anchovy eggs and larvae downstream towards the south-east end, off Cape Passero, where larvae are retained in a frontal structure that originates from the meeting of AIS and Ionian Sea water masses (García Lafuente *et al.*, 2002). Its path and its year-to-year variability have consequences for the other predominant hydrological phenomena occurring in the region, such as the extension of upwelling and the formation of frontal structures. If the AIS path moves further offshore, the northern coasts can show a greater upwelling extension, thereby modifying the temperature regime of the surface waters, cooling them below the optimal temperatures for anchovy spawning, which is 19–23°C and the normal temperature range in anchovy spawning grounds off the west Mediterranean basin during summer, when peak spawning takes place (June to July) (García and Palomera, 1996).

Local or larger scale fisheries studies aiming to analyse environmentally driven stock fluctuations need time series of environmental variables causing hydrographic variability, such as wind stress, water temperature, wind curl and atmospheric pressure. Other important oceanographic structures that may act as driving forces affecting the habitat of the species and recruitment variability are more difficult to monitor. For instance, oceanographic fronts, which are favourable reproductive habitats for many fish species including small pelagics (Bakun, 1996; Agostini and Bakun, 2002), belong to this category. Fronts change in shape, position and intensity (defined as the size of the horizontal cross-front gradient of a given variable) with time and there is no single variable to describe their variability. An important issue is to define potential indicators that could be used as rough quantifiers of the temporal variability of complex environmental structures, such as oceanographic fronts. Most fronts have distinguishable thermal contrast at the sea surface and can be easily detected from satellite-derived sea surface temperature (SST) which has become a fundamental variable in earth science, including fisheries oceanography (Simpson, 1994).

The technique of ‘spatial’ empirical orthogonal functions [(EOF), also known as principal component analysis; Hotelling, 1933; Preisendorfer, 1988] applied to SST images has proved to be useful for detecting

structures with SST spatial gradients like fronts or eddies (Lagerloef and Bernstein, 1988; Vargas *et al.*, 2003). Spatial EOF analysis has the potential to extract the variance associated with these features into a few modes of variability and to give its spatial pattern and time variability. In this paper, EOF analysis of SST is used to characterize complex environmental features influencing the early life stages of the anchovy in the northern area of the Sicilian Channel. This area was recently identified as containing important regional-scale ‘ocean triads’ (Agostini and Bakun, 2002), a concept introduced by Bakun (1998) to describe environmental requirements for the survival of small pelagic fish. Knowledge of the main hydrographic features of the region and the way these interact with the life cycles of the fish species is necessary to establish adequate relationships between these potential environmental indicators and the key stages of the life cycle of the anchovy. SST time series can only be used with this aim if these hydrographic features exhibit thermal surface signatures, as shown here. The EOF technique is applied to the time series of SST images of the Sicilian Channel and the temporal coefficients of the dominant empirical modes are investigated as potential indicators of the variability at different time scales of surface structures affecting the reproductive cycle of the Sicilian anchovy.

#### *Regional hydrography*

The surface circulation of the two-way exchange flow through the Sicilian Channel is the main point of interest for this study. The principal hydrodynamic feature is the existence of the along-channel, meandering current of Atlantic origin, the AIS (Robinson *et al.*, 1999). Figure 1 identifies the most important hydrographic structures found in the Sicilian Channel and its approaches. The AIS encircles two cyclonic vortices over Adventure Bank [Adventure Bank Vortex (ABV); toponyms follow the works of Lermusiaux, 1999; Robinson *et al.*, 1999; Lermusiaux and Robinson, 2001] and off Cape Passero [Ionian Shelf Break Vortex (IBV)] and describes a pronounced anticyclonic meander in between [Maltese Channel Crest (MCC)]. A third cyclonic vortex [Messina Rise Vortex (MRV)] is sometimes found on the eastern side of Sicily, south of Messina strait (Lermusiaux, 1999). Other important features are the so-called Ionian slope fronts (ISFs; Lermusiaux, 1999) located at the eastern boundary of IBV and MRV and running further south along the Ionian slope. According to Lermusiaux and Robinson (2001), the fronts prevail at different locations and depths. The uppermost is temperature dominated because of the advection of Modified

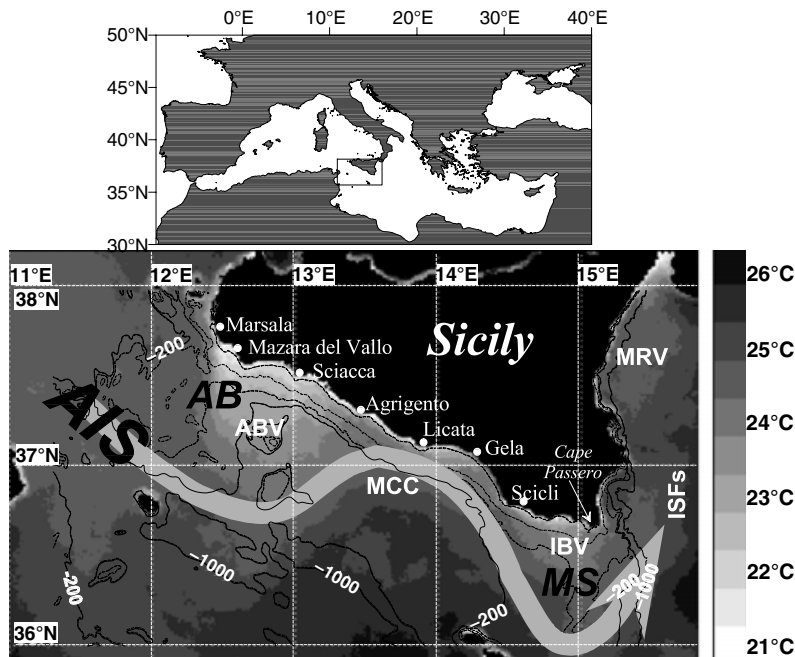


**Figure 1.** Main topographic and hydrographic features of the Sicilian Channel superposed on a monthly averaged SST image of June 1988. The white winding arrow depicts the trajectory of the AIS according to Robinson *et al.* (1999). Depth contours of  $-200$  m and  $-1000$  m have been labelled. Non-labelled contours are  $-100$  m and  $-50$  m. AB, Adventure Bank, and MS, Maltese Shelf, are labelled in black. White labels indicate the main surface structures: ABV, Adventure Bank Vortex; MCC, Maltese Channel Crest; IBV, Ionian Shelf Break Vortex; MRV, Messina Rise Vortex; ISFs, Ionian Shelf Fronts.

Atlantic Water (MAW) by the AIS, while the deeper one is salinity dominated, because of the topographically forced rise of salty Levantine Intermediate Water (LIW) by the Ionian slope. In the upper part of the water column, both fronts overlap and act in opposite senses, with the resulting surface density front still being dominated by temperature north of  $36.3^{\circ}\text{N}$  (Lermusiaux and Robinson, 2001).

All these structures are identifiable in the SST map of Fig. 1: the cyclonic vortices by their cold surface signature, the MCC by the intrusion of warm water to the shore in between ABV and IBV, and the ISFs by the strong zonal SST contrast around  $16^{\circ}\text{E}$ . Among these structures the MCC, the IBV and the ISFs are of particular interest because of their influence on the life cycle of the Sicilian Channel anchovy.

The simplified circulation sketched in Fig. 1 fluctuates at different time scales, from a few days, associated with the pass of weather systems (Manzella *et al.*, 1990), to seasonal and interannual scales associated with variations in the MAW and LIW transports through the Sicily Channel (Pinardi *et al.*, 1997; Astraldi *et al.*, 1999). According to García Lafuente *et al.* (2002), anchovy spawning preferably occurs in the area where AIS approaches the coast (MCC). Therefore, the interannual variability of trajectory of the AIS influences the environmental conditions of the anchovy spawning habitat. The changes of the AIS trajectory enlarges or reduces the area occupied by the cyclonic vortices and displaces the MCC offshore/onshore or/and north-west/south-east. This, in turn,

changes the location and extent of the Sicilian coast washed by the AIS, which is a critical factor in determining the position of the main spawning grounds of the Sicilian anchovy (García Lafuente *et al.*, 2002). For instance, an offshore-located AIS path increases the size of the ABV and modifies the temperature regime of the surface waters in the habitat of the Sicilian anchovy. In this case, these waters would be below the optimal temperature range for Mediterranean anchovy spawning, between  $19$  and  $23^{\circ}\text{C}$  during its spawning peak (June to July; García and Palomera, 1996). The converse would occur if the AIS approximates the coast.

This study is intended to provide an exploratory tool for assessing hydrographic variability of key driving forces that may affect recruitment oscillations of small pelagics. As such, one of the key processes that influence anchovy spawning habitat variability is the year-to-year variability of the AIS trajectory. The EOF applied to SST images has the potential to monitor hydrographic interannual fluctuations, if these have thermal signatures.

## MATERIAL AND METHODS

### *Hydrographic and biological data*

Field data were acquired during three oceanographic surveys carried out in June to July of 1998, 1999 and 2000 respectively. The hydrographical data set (CTD casts) was collected with a Sea-Bird 25 CTD probe

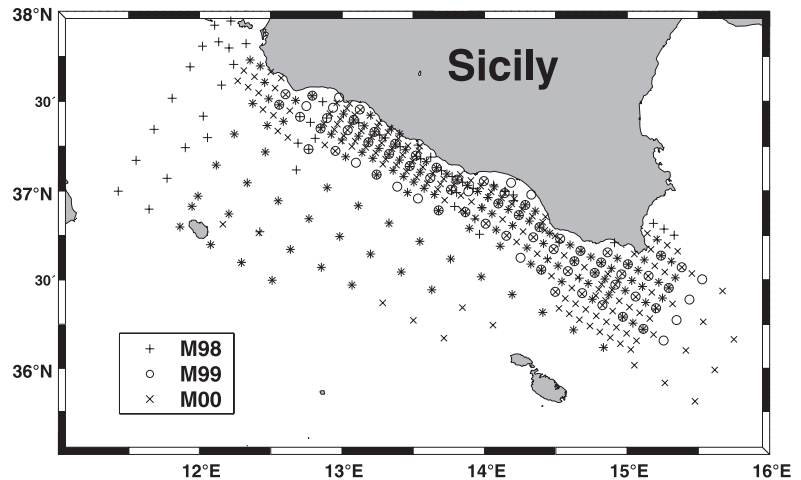


**Figure 2.** Grid stations in the surveys M98, M99 and M00.

onboard the *R/V Urania* in 1998 and 2000 (surveys M98 from 24 June to 11 July 1998, and M00 from 23 June to 13 July 2000, respectively) (see Fig. 2) and with a SBE911 CTD probe onboard the *R/V Cooper-naut Franca* in 1999 (M99 from 19 to 25 June 1999). An exhaustive analysis of these hydrographical data sets is available in Mazzola *et al.* (2002).

To assess anchovy egg and larval distributions, vertical CalVET (25-cm diameter, 150- $\mu\text{m}$  mesh) and oblique Bongo 40 (40-cm diameter, 200-mm mesh) plankton tows were carried out. Both types of plankton hauls covered the 100-m depth, whenever possible. All plankton samples were fixed and preserved in a 5% buffered Formalin solution. All counts were standardized to numbers per 10 m<sup>2</sup>.

#### SST data

The data set consists of 404 weekly composite SST images from February 1993 to November 2000, derived from NOAA/AVHRR infrared sensor data. They were downloaded from the German Remote Sensing Data Centre web site, which offers daily, weekly and monthly SST maps based on multiple daily passes with a maximal spatial resolution of 1.1 km. The selected spatial coverage of the images is 35°30'N–38°0'N and 11°0'E–15°1'E.

To minimize the effect of clouds on the EOF analysis, images with more than 10% cloudy sea pixels were rejected, thereby reducing the final number of available images to 363. In the non-rejected, but still cloudy, images, the mean temperature of the non-cloudy sea pixels was assigned to the cloudy pixels. This preserves the spatial mean of the temperature but introduces short-scale spurious structures which will be mainly captured by the less important, high-order EOF modes. The dominant modes, which capture large-scale spatial structures, will not be influenced by this

procedure. Nevertheless, a  $3 \times 3$  spatially weighted filter was further applied to minimize the effect of this and other sources of short-scale spatial noise (Wang *et al.*, 1983). The filter was applied wherever no ground pixels were inside the filter window. Otherwise, the corresponding pixel of the filtered image was set to zero, the coded value for ground. Filtered images were subsampled to a spatial resolution of 3.3 km.

The rejection of cloudy images creates an uneven spacing of images in the SST series. This unevenness is not important for EOF analysis but it may introduce some slight bias towards summer conditions, when cloudy images are less frequent. Most of the gaps (80%) in the final SST time series were of just one image and the remaining 20% of two images.

The EOF analysis provides information on time variability through the time coefficients of the modes. To analyse the full range of time variability it is usual to separate the different time scales by means of numerical filters. An order 8 low-pass Butterworth filter with half power cut-off frequency of 0.0078 day<sup>-1</sup> (or 4.2-month period) was used to separate 'low' and 'high' frequency signals. Gaps in the SST series, which are transmitted to the series of the time coefficients, were linearly interpolated to obtain a constant sampling interval and to facilitate the filtering.

#### Meteorological data

Six hourly air temperature, pressure and wind velocity data, for Trapani, Gela and Cape Passero in southern Sicily over the same time span as the SST data set were provided by the Aeronautica Militare Service (Italy). The observations were smoothed by a Gaussian-like filter of 1 cpd cut-off frequency and decimated to a sample per day. The resulting series were then weekly averaged in order to have the same sampling interval

and averaging as the SST time series. The meteorological data sets were used to test for correlations between the empirical modes and the atmospheric forcing. The monthly North Atlantic Oscillation index, based on Gibraltar and Iceland atmospheric pressure observations (Jones *et al.*, 1997), was used.

#### Empirical orthogonal function analysis

Spatial EOF analysis, first suggested by Lagerloef and Bernstein (1988), was implemented in this work. Let us consider the spatially demeaned SST  $T(r_i, t_j)$

$$T(r_i, t_j) = T_o(r_i, t_j) - \frac{1}{M} \sum_{i=1}^M T_o(r_i, t_j) \quad (1)$$

where  $T_o(r_i, t_j)$  is the measured SST at position  $r_i$  ( $i = 1 \dots M$ , the number of sea pixels) and time  $t_j$  ( $j = 1 \dots N$ , the number of images). They can be arranged as a matrix  $T$  of  $M \times N$  elements ( $N$  images – columns of  $M$  sea-pixels each). The  $N \times N$  covariance matrix  $C$  associated with these data is

$$C = \frac{1}{M} (T^T \cdot T) \quad (2)$$

whose elements are the covariance between spatially demeaned images. EOF analysis seeks a set of spatial functions  $\phi_k$  and time coefficients  $b_{jk}$  such that the ‘reconstructed’ SST image

$$T_j \cong \sum_{k=1}^P b_{jk} \phi_k \quad j = 1, \dots, N \quad (3)$$

with  $P \leq N$  fulfils the condition that, for any  $P$ , the mean squared error

$$\varepsilon = \sum_{j=1}^N \left\langle \left| T_j - \sum_{k=1}^P b_{jk} \phi_k \right|^2 \right\rangle \quad (4)$$

over the entire set is minimized (brackets denote spatial average). This minimization problem leads to a set of  $N$  eigenfunction equations of the form (Sirovich and Everson, 1992)

$$C \phi_k = \lambda_k \phi_k \quad k = 1, \dots, N \quad (5)$$

from which the  $N$  eigenvalues,  $\lambda_k$ , and  $N$  eigenfunctions or empirical modes,  $\phi_k$ , are easily computed.

## RESULTS AND DISCUSSION

### Surface temperature and anchovy egg and larval spatial distribution

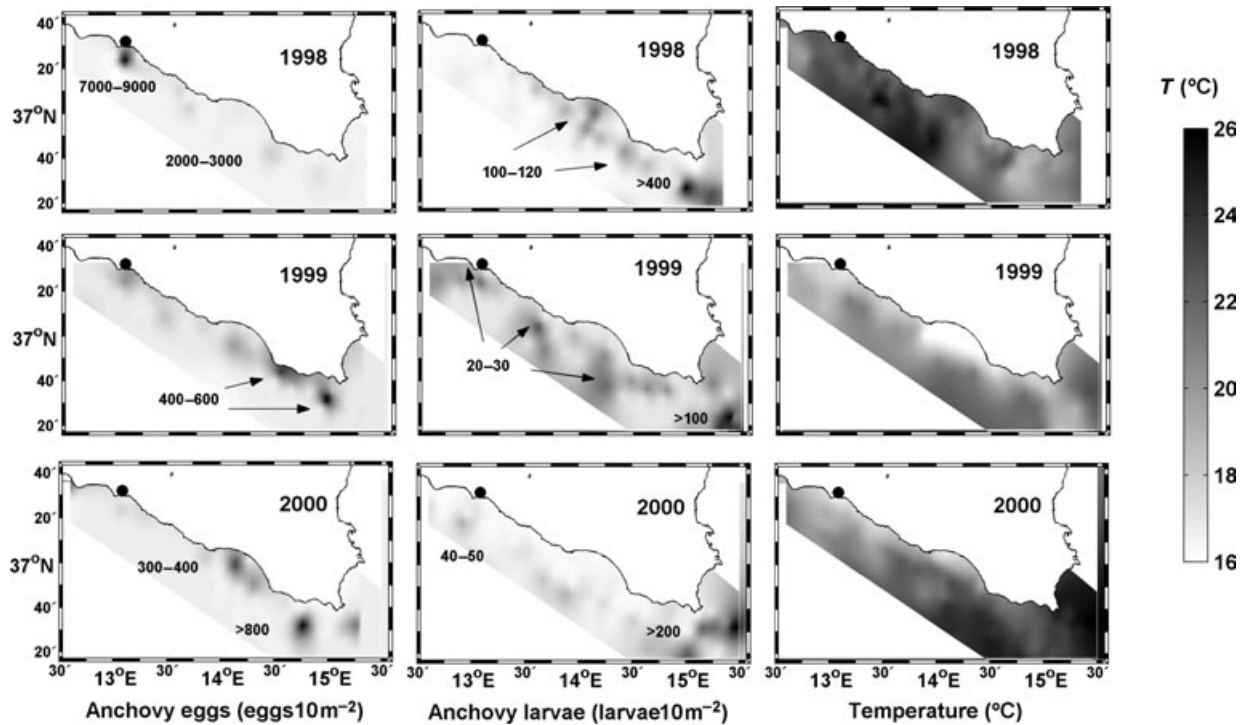
The spatial distribution of anchovy eggs and larvae from the surveys M98, M99 and M00 and the distribution of the respective surface temperatures shows a clear relationship. Although the anchovy spawning grounds may spread over the southern Sicilian coast to a depth of 100 m (left panel of

Fig. 3), the study of Mazzola *et al.* (2002) showed that the bulk of the anchovy stock and the principal fishing grounds were located within the narrow shelf between Sciacca and Gela (Fig. 1).

Nevertheless, marked interannual variability was observed in the location of the main spawning grounds and the observed egg abundances. A comparison of the spatial distribution of egg abundance and the water temperature at the uppermost metres (right panel of Fig. 3) shows increased egg abundance in areas of higher surface temperatures. M98 survey, which recorded the highest temperature of the survey series and was on average  $\pm 1.5^\circ\text{C}$  higher than in 1999 and 2000 (Mazzola *et al.*, 2002), observed anchovy egg abundances one order of magnitude greater (maximum density of 9300 eggs per  $10 \text{ m}^2$  in 1998 in comparison with 600 eggs per  $10 \text{ m}^2$  and 970 eggs per  $10 \text{ m}^2$  in 1999 and 2000, respectively; see Fig. 3). Likewise, 1998 rendered the highest estimated spawning biomass through the Daily Egg Production Method (13 224 MT in 1998 in comparison with 3010 and 2850 MT in 1999 and 2000) (Quintanilla and García, 2001a; Mazzola *et al.*, 2002).

Fishery catch data indicate that the fishing grounds of Sicilian anchovy is the narrow shelf that extends from Sciacca to Gela (see Fig. 1 for location), although the main bulk of the stock is located off the coasts of Sciacca (Mazzola *et al.*, 2002). Based on this fact, the spatial patterns in Fig. 3 are interpreted as follows: when surface temperature in the area where reproductive adults concentrate is high, spawning activity is also very high, as in 1998. When temperature in the main fishing ground off Sciacca is low, the reproductive adults in this area show a high incidence of atretic stages of oocytes (oocyte resorption) and sexually inactive females (Quintanilla and García, 2001b; Mazzola *et al.*, 2002), reducing the spawning activity. Egg distributions during the years of cold surface water off Sciacca indicate that spawning occurs preferably in the southern coasts with higher temperature (Fig. 3) but with fewer reproductive adults. Consequently, the overall spawning diminishes. This temperature-related reproductive behaviour was especially evident during 2000, when some adult anchovy samples collected off Sciacca recorded as much as 20% of anchovies in atretic stages and over 40% of specimens sexually inactive. The high incidence of atretic and/or inactive females during the peak spawning season cannot be attributed to the termination of spawning, but to unfavourable environmental conditions (Quintanilla and García, 2001b; Mazzola *et al.*, 2002).

**Figure 3.** Panels on the left, from top to bottom, are anchovy egg distributions during M98, M99 and M00 surveys, respectively. Numbers are egg concentration where local maxima were found. Central panels are anchovy larva distributions during the same surveys. Numbers are as in left panels. Right panels show the average temperature of the upper 10 m. The black dot in the southern coast of Sicily near 13°E indicates the main fishing port of Sciacca.



Most of the southern Sicilian coast is under the influence of ABV and IBV, which have cold surface signatures (Fig. 1) and only the area between these vortices may be under the influence of warmer MAW, advected by the AIS (MCC feature in Fig. 1). Two different hydrographic scenarios may occur: if MCC is closer to the coast, then the area where the main anchovy stock is distributed is invaded by warm water; and secondly, if MCC is displaced towards the south/south-east, this area remains under the influence of the colder ABV, thereby causing an unfavourable temperature decrease for anchovy spawning. Figure 3 shows that the first situation prevailed during M98 and the second during M99 and M00.

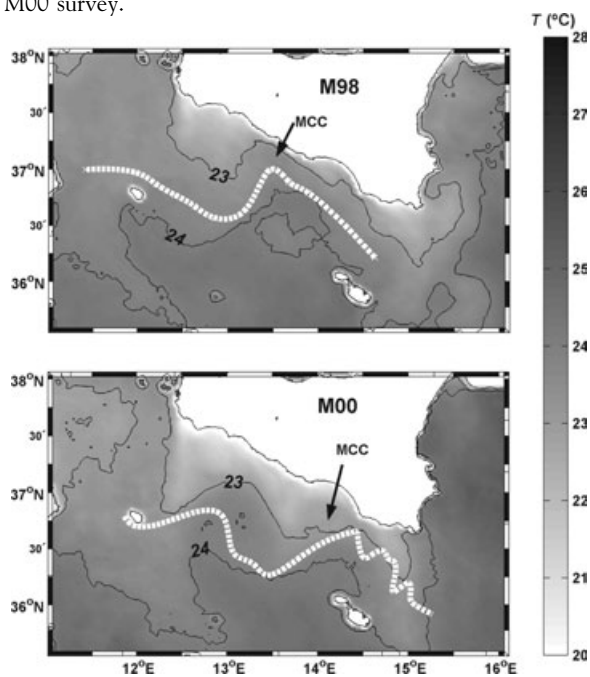
Whatever the anchovy egg distribution along the southern coast of Sicily is, the larvae tend to concentrate off Cape Passero because of the AIS advection (García Lafuente *et al.*, 2002) (central panels of Fig. 3). Off Cape Passero, the presence of the surface ISFs is able to provide a suitable scenario of enrichment, concentration and retention (the fundamental triad; Bakun, 1996), and, thus form a favourable nursery habitat for anchovy larvae, as well as for other pelagic species (Mazzola *et al.*, 2002).

#### *Thermal signatures of the surface circulation*

In the model described above, the path of the AIS ultimately influences the overall abundance and distribution of anchovy eggs and the concentration of larvae off Cape Passero. Therefore, its associated interannual variability plays a significant role in the spawning strategy of the Sicilian anchovy. The distinguishable thermal signature of the AIS and ISFs, particularly in summer when spawning occurs, indicates the potential of SST to provide an index of environmental conditions during key moments of the early life stages of anchovy.

To further test the reliability of SST to describe the AIS path in the Sicilian Channel, hydrographic data were used to find the salinity minimum at each meridional CTD transect. This minimum is the MAW signature that was used to track the core of the AIS along the Channel. Figure 4 shows the satisfactory agreement between the time-averaged SST images during M98 and M00 surveys and the trajectory of the AIS deduced by the core method; the 23–24°C isotherms represent the AIS well. The agreement allows the use of SST to estimate the variability of the AIS

**Figure 4.** (a) Average SST during M98 oceanographic survey. The dashed line shows the path of the AIS inferred by the minimum salinity core technique. (b) Same as (a) for M00 survey.



trajectory, which was carried out by means of EOF analysis.

#### Results of EOF analysis

Table 1 shows the percentage of variance of the SST data set explained by each of the three first empirical modes. Modes >3 explain <3% of the variance and are not considered here.

Figure 5 presents the spatial maps of these leading modes normalized by  $(\lambda_k)^{-1/2}$  in order to have them dimensionless and with unit variance. The time coefficients,  $b_{jk}$ , were re-scaled by the factor  $(\lambda_k)^{1/2}$  in order to maintain the product  $b_{jk}\phi_k$  in eqn 3 unaltered. They have a dimension of temperature and are presented in Figs 6a–c. Figure 6d shows the time series of the spatially averaged SST that was subtracted from the analysed images (and that must be added to eqn 3 in order to recover the actual temperature field).

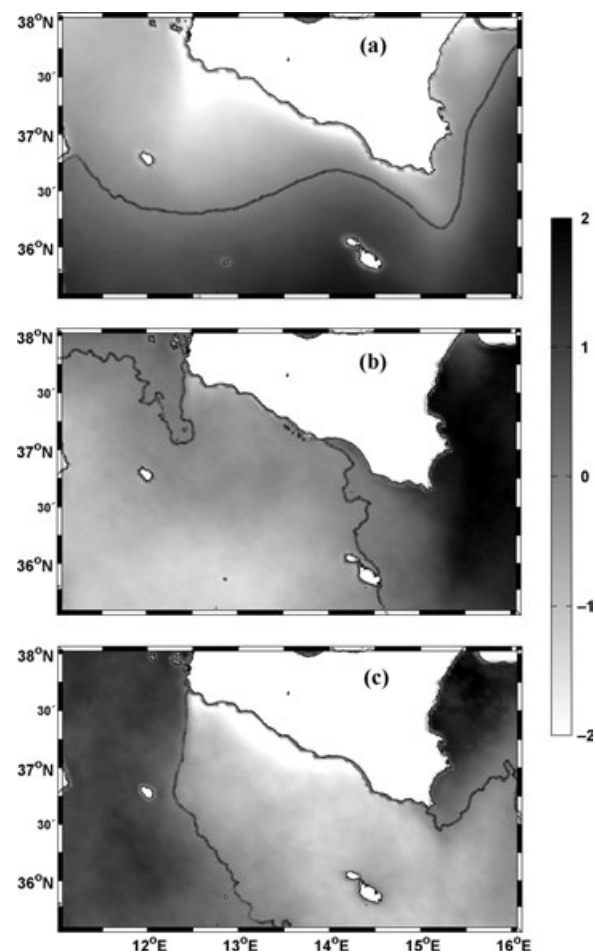
**Table 1.** Percentage of variance and cumulated variance explained by the first three empirical modes.

Mode	% Variance	% Cumulated variance
1	47	47
2	12	59
3	7	66

The spatial map of mode 1 (Fig. 5a) resembles the main circulation of the AIS sketched in Fig. 1. The cool signatures of the ABV, IBV and, to a lesser extent, of MRV are easily recognizable. This mode contains almost half the total variance (Table 1), indicating that much of the Sicilian Channel variability is associated with changes in the AIS, also shown by Lermusiaux (1999). Time coefficients of this mode do not change sign (Fig. 6a), which implies that the thermal gradients shown in Fig. 5a do not reverse.

The most noticeable feature of the spatial pattern of mode 2 (Fig. 5b) is the line of zero amplitude that runs from Cape Passero southwards, separating two regions of opposite sign in the location where the northern part of the ISFs are usually found. Its time coefficients (Fig. 6b) fluctuate near zero and change sign frequently with seasonal modulation. Temperature gradients in the spatial map (Fig. 5b) change sign accordingly.

**Figure 5.** Spatial map of mode 1 (a), mode 2 (b) and mode 3 (c) normalized to unit variance. Dashed line indicates the zero-value. Contours are dimensionless (see text).



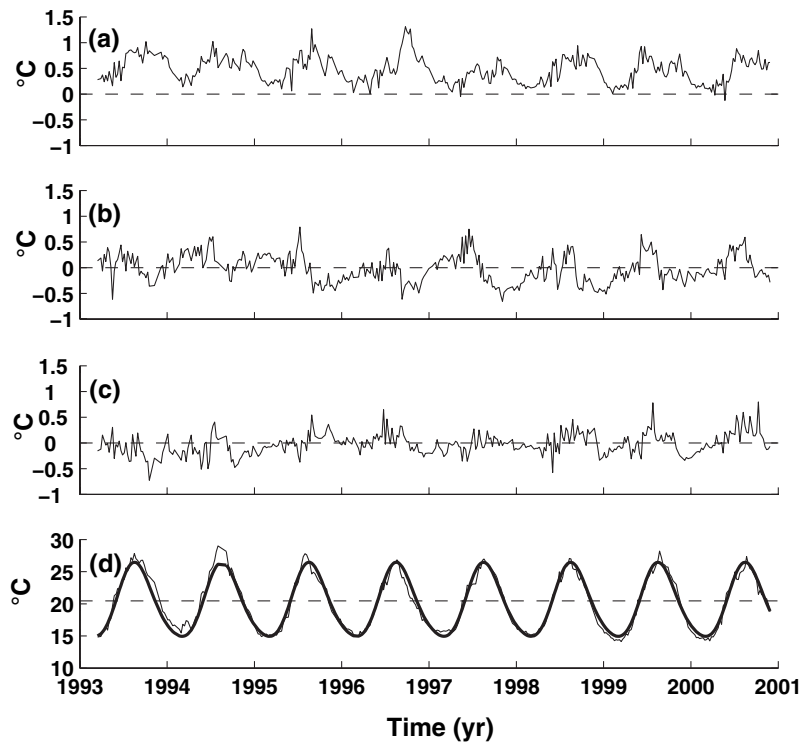


**Figure 6.** Time coefficients of mode 1 (a), mode 2 (b) and mode 3 (c), re-scaled by the factor  $(\lambda_k)^{1/2}$ . (d) The time series of the spatially averaged temperature in the area (thin line). Thick line is the seasonal fitting of the series to eqn 6.

The spatial structure of mode 3 (Fig. 5c) has a notable offshore amplitude gradient off the southern coast and a high amplitude in the eastern part of Sicily at the MRV. The time coefficients also have nearly zero mean (Fig. 6c) and frequent sign changes.

The temporal coefficients of these modes fluctuate at different time scales. The shortest time scale resolvable is fortnightly, the Nyquist frequency of 1-week sampling, while an almost 8-yr time series allows the analysis of interannual variability. The annual (seasonal) cycle plays an important role in the temporal variability (Fig. 6), although the shorter period fluctuations also capture a considerable amount of the variance. For this reason, the different contributions were separated by the numerical Butterworth filter previously described, which leaves annual and interannual variability in the low-passed series and shorter scale (mesoscale) variability in the high-passed series (Figs 7 and 8).

#### Seasonal variability

There are two types of seasonal variability. The first, shown in Fig. 6d, is the spatially constant SST that follows the annual solar cycle. It does not have dynamic importance because it does not generate spatial gradients. The second type affects the spatial maps through the variability of the time coefficients. To numerically characterize the signal, the time

coefficients series shown in Fig. 7 were fitted to the model

$$f_k(t) = A_0 + A_a \cos(\omega_a t - f_a) + A_s \cos(\omega_s t - f_s) \quad k=0,1,2,3 \quad (6)$$

where  $A_0$  is the mean and  $\omega$ ,  $A$  and  $f$  are frequency, amplitude and phase (referred to the first day of the year) of the annual (subindex  $a$ ) and semi-annual (subindex  $s$ ) signals, respectively. Index  $k=0$  is for the spatially averaged temperature. Table 2 shows the result of the fitting and indicates that 40–70% of the variance of the low-passed series is accounted for by these seasonal signals.

The annual ( $\omega_a$ ) signal of the fitted time coefficients of mode 1 peaks in year-day 257 ( $f_a = 254^\circ$ , 14 September), but the small contribution of the semi-annual ( $\omega_s$ ) signal displaces the absolute maximum to the end of September. Thermal gradients of Fig. 5a are maximum on those dates and are greatly reduced in March, when the time coefficients are at their lowest values. Should mode 1 represent the AIS path realistically, the flow associated with this stream would have similar seasonal fluctuations. Time coefficients of mode 2 have smaller annual and greater semi-annual amplitude than those of mode 1, distorting the sine curve to the shape shown in Fig. 7b, with maximum values by the end of June. On these days, the thermal front off Cape Passero

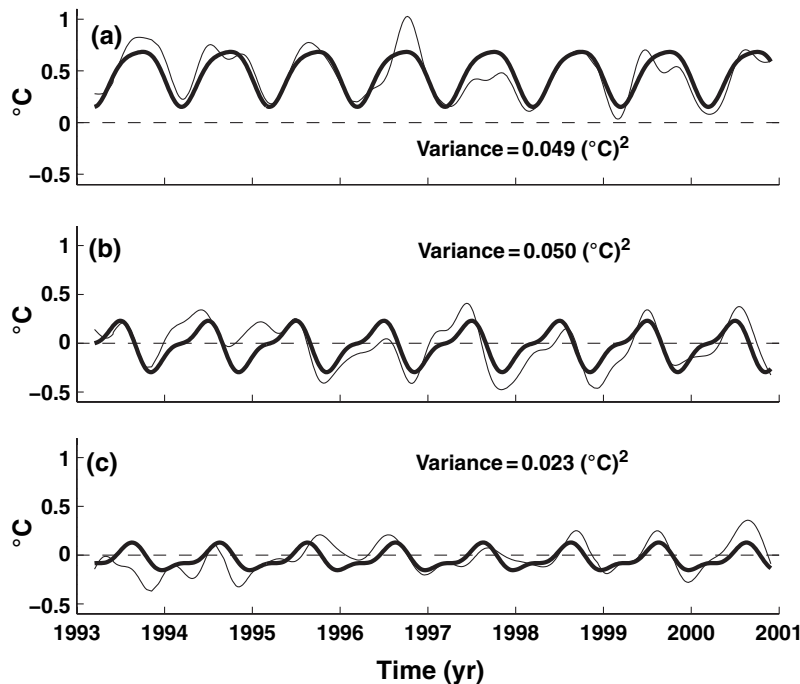


**Figure 7.** Low-passed series (thin lines) of the time coefficients of mode 1 (a), mode 2 (b) and mode 3 (c). Thick lines are the fitting of the series to eqn 6. The variance of the low-passed series is indicated in each plot.

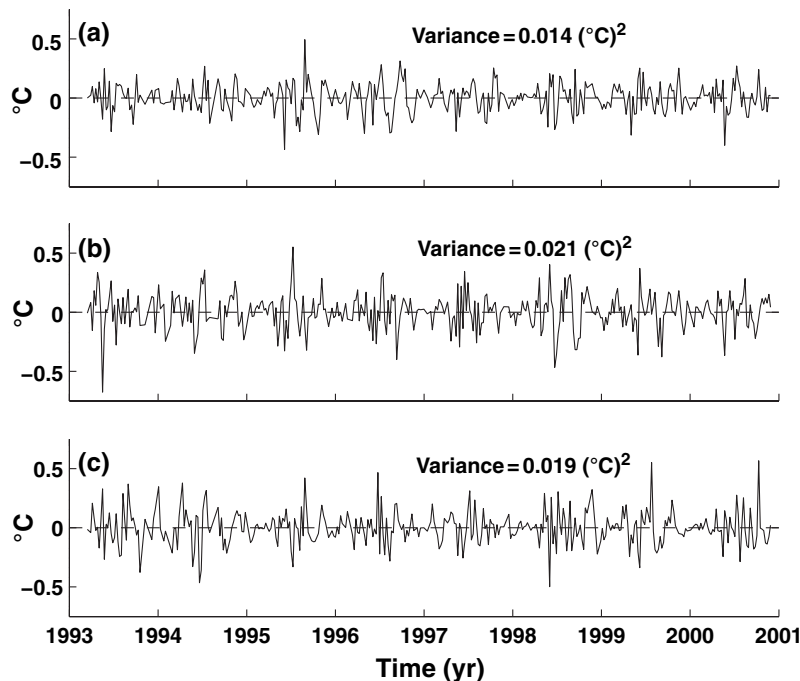


**Figure 8.** High-passed series of the time coefficients of mode 1 (a), mode 2 (b) and mode 3 (c). The variance of the series is indicated in each plot.

(Fig. 5b) is enhanced. In autumn-winter, the time coefficients are negative, causing the reverse of thermal gradients represented by this mode. Seasonal signal in the time coefficients of mode 3 is lower than in modes 1 and 2 but still significant. It tends to peak by mid-August and is minimal by the end of the year. Thermal

signatures in Fig. 5c would be enhanced in summer, particularly for the warm pool of water in the eastern part of Sicily near the MRV and the cross-shelf contrast in the south of Sicily.

The final SST map at any time is the linear combination of all the empirical modes (eqn 3). The

**Table 2.** Parameters of eqn 6, and their 95% confidence intervals for the three first empirical modes shown in Fig. 4. Columns 2, 3 and 4 are the mean, annual and semi-annual amplitudes, respectively, and columns 5 and 6 are the annual and semi-annual phases, respectively. Last column is the regression coefficient.

Mode	$A_0(^{\circ}\text{C})$	$A_a(^{\circ}\text{C})$	$A_s(^{\circ}\text{C})$	$f_a(^{\circ})$	$f_s(^{\circ})$	$r^2$
1	$0.46 \pm 0.04$	$0.26 \pm 0.05$	$0.05 \pm 0.05$	$254 \pm 12$	$311 \pm 66$	0.69
2	$-0.03 \pm 0.04$	$0.22 \pm 0.06$	$0.09 \pm 0.06$	$149 \pm 15$	$37 \pm 39$	0.61
3	$-0.03 \pm 0.03$	$0.12 \pm 0.05$	$0.05 \pm 0.05$	$212 \pm 23$	$108 \pm 48$	0.40

former discussion describes each of the first three terms in eqn 3 independently, which could lead to misleading conclusions. For instance, a negative time coefficient of mode 2 implies the change of sign of the thermal gradient off Cape Passero associated with this mode (Fig. 5b), which in turn could suggest colder water in the Northern Ionian Sea than in the Channel. The real map must contain the contribution of the remaining modes, especially mode 1, which prevents the inversion of the temperature gradient. This can be better observed in Fig. 9, which shows 12 monthly SST maps generated through eqn 3, with  $k = 1, 2, 3$  and the time coefficients computed with the parameters of Table 2 on the central day of each month from eqn 6. The spatially averaged temperature of Fig. 6d has not been included in order to have a unique and suitable grey scale for all maps (strictly speaking, Fig. 5 shows temperature departures from the spatially averaged monthly mean).

In Fig. 9, the seasonal signal of mode 1 time coefficients is easily recognized in that the temperature gradient across the AIS trajectory is greatly enhanced in summer (cooler water over Adventure Bank). This would imply the enhancement of the AIS flow in the case where salinity does not determine the density gradients. It does not agree with dynamic studies of this area, which show maximum transport and kinetic energy of the AIS in winter in response to more vigorous wind stress and reduced stratification (Manzella *et al.*, 1990; Onken and Sellschopp, 1998). Therefore, surface thermal structures must be interpreted with care when exploring their meaning. Fortunately, these structures correlate well with the path of the AIS in summer (Robinson *et al.*, 1999; see also Fig. 4), a fact that supports the dynamic interpretation of SST patterns, at least during this season. The thermal front off Cape Passero is enhanced from May to August, showing the greatest contrast in June to July, when mode 2 time coefficients peak. It suggests that these coefficients are useful indicators of the time evolution of the front. Notice, however, that the final shape of the front is achieved by the combination of modes 1 and 2, the former being responsible for the thermal

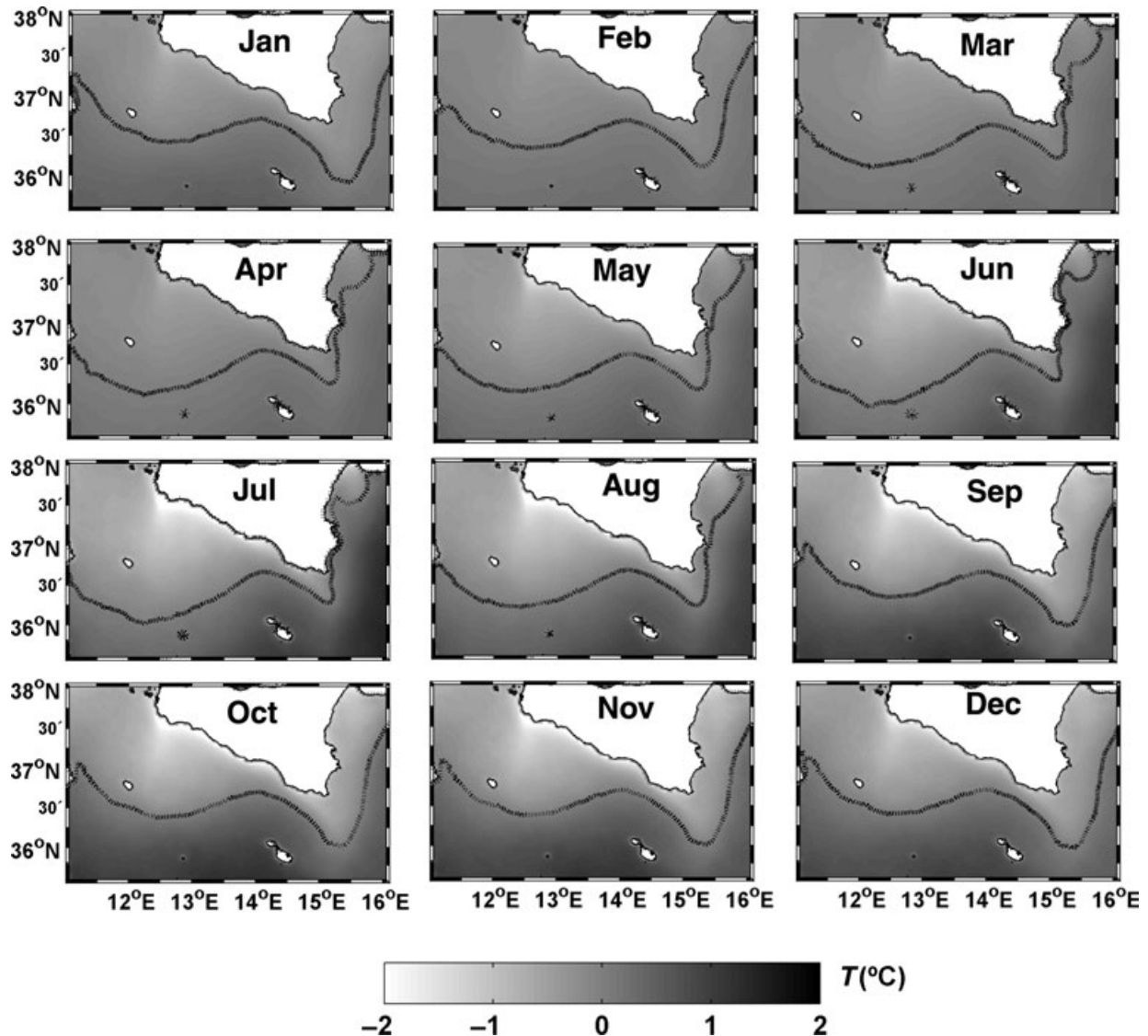
gradients not changing across the front throughout the year and mode 2 changing these gradients. Mode 3 contribution to the seasonal cycle is harder to detect because of the smaller amplitudes of the signals (Table 2); the enhancement of the cool signature of the MRV east of Sicily is its contribution to Fig. 9.

#### Mesoscale and interannual variabilities

The variance of the low- and high-passed series of the time coefficients for mode 3 is similar (see inserts in Figs 7 and 8), while mesoscale (high-passed) contribution is of secondary importance for modes 1 and 2. The time coefficients of mode 3 can be up to four times greater than the annual amplitude of this mode (see Table 2 and peaks in Fig. 8c). Figure 10 shows the impact of such events on SST maps. Figure 10a shows a mean June to July situation using modes 1 and 2. The dashed line that runs along the 0 contour roughly represents the AIS trajectory in the following discussion. Figure 10b: the spatial map of mode 3, multiplied by a positive time coefficient of three times its annual amplitude (Table 2), were superimposed on Fig 10a. The dashed line has been displaced to the south, making the AIS approach the Sicilian shore farther to the south-east. Figure 10c is modified from Fig. 10a by superposing the third mode multiplied by a negative coefficient of three times its annual amplitude. The MCC of the AIS is displaced towards the north, shrinking the ABV and IBV vortices and flooding the main fishing grounds off Sciacca with warm water. The time coefficients of mode 3 can detect these displacements and, therefore, become potential indicators of environmental conditions during a key period of the anchovy reproductive cycle.

Interannual variability of environmental conditions during the anchovy spawning season is of particular interest. It was analysed by removing the seasonal signal from the low-passed time series and adding the mesoscale variability (Fig. 11a–c). This correction is justified because mesoscale variability may modify the shape of the slowly varying inter-annual signal during the limited period of spawning. A June-averaged value was computed and considered

**Figure 9.** Synthesized monthly SST maps using the three first empirical modes and the time coefficients at the central day of each month. The time coefficients used come from the seasonal fitting of eqn 6.



as representative of the time coefficients of the modes during the spawning period. In June 1998, the time coefficient of mode 3 was very negative, which indicates a shoreward displacement of the AIS and consequently, warm water over the main fishery ground during M98 (see also Fig. 4a). In June 1999 and 2000, the time coefficients of mode 3 were clearly positive implying a trajectory of the AIS far offshore from the Sicilian coast, a situation also depicted in Fig. 4b for year 2000.

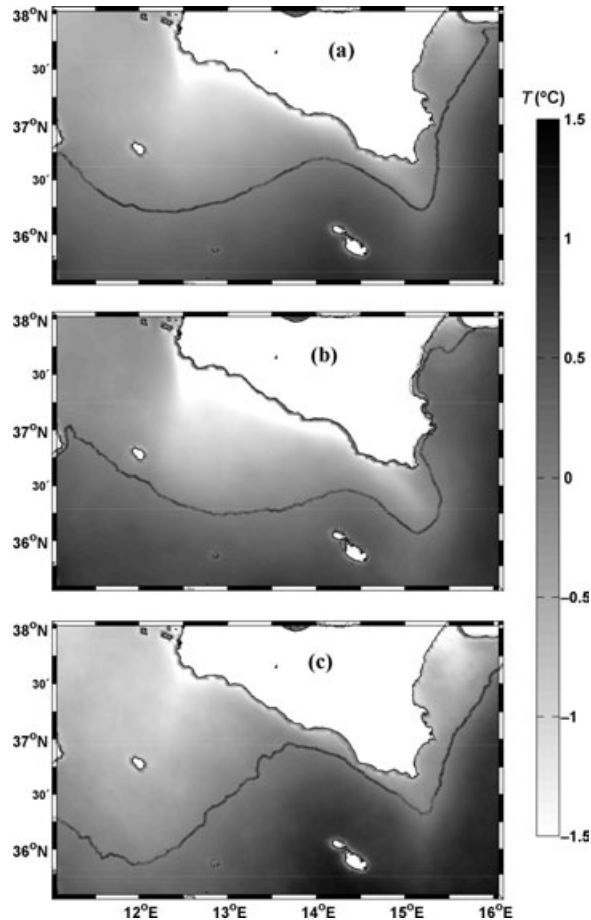
The other important hydrographic feature with influence on the early life stages of the Sicilian anchovy is the front off Cape Passero. Time coefficients of modes 1 and 2 in 1999 showed strong

positive anomalies in the same direction, enhancing the thermal front. A strong surface temperature front was present in the upper 20 m of the water column during the M99 survey (Fig. 12, central panel). The front during years 1998 and 2000 was not so strong (upper and lower panels of Fig. 12), consistent with the negative values of modes 1 and 2 coefficients in June 1998 and their near-zero values observed in June 2000.

#### *Physical forcing*

Another issue to be addressed is the relationship of the empirical modes to external forces. At the seasonal scale, the annual solar cycle is the main driving force

**Figure 10.** (a) SST map generated with modes 1 and 2 for June to July. (b) SST map of (a) modified by the contribution of mode 3 weighted with a positive time coefficient of  $+0.4^{\circ}\text{C}$ . (c) SST map of (a) modified by the contribution of mode 3 weighted with a negative time coefficient of  $-0.4^{\circ}\text{C}$ . Dashed lines run along the 0 contour and are indicators of the AIS trajectory.



and is likely responsible for the seasonal signal detected in all modes. Neither of them is able to capture the overall externally forced seasonal variance. The surface patterns appear too complex to be explained by a single mode. The same external agent excites more than one EOF as shown in this case, which means that a combination of empirical modes can be more significant than a single mode in order to explain some features. An example of this is the intensification of ISFs in summer, explained by the combination of modes 1 and 2 time coefficients, which are more sensitive to the seasonal signal than mode 3 (Table 2).

In addition to the seasonal variability, mesoscale and interannual variability remains after the seasonal signal is removed. To investigate their relation to

external forces of meteorological origin, the meteorological time series were processed the same way as the EOF time coefficient series. That is, a seasonal signal has been identified through eqn 6 and removed from the original series and the resulting series have been separated in low (interannual) and high (mesoscale) frequencies by means of the Butterworth filter. Table 3 shows the results of the correlation analysis for low- and high-passed bands. Only the significant correlations highlighted in the table are discussed.

Mode 1 is negatively correlated to the air temperature anomaly at low frequency. The cooler the year (negative anomaly), the higher the thermal gradients are in the spatial map of mode 1 (Fig. 5a). We speculate that negative air temperature anomalies cause stronger sea-air heat fluxes, which in turn increase buoyancy losses and deep water formation and, hence, enhance the thermohaline circulation in the Mediterranean. Stronger AIS flow would be needed to compensate for the extra deep convection in the eastern Mediterranean, manifested by enhanced thermal gradients in the Channel.

The low frequency contribution of mode 2 is positively correlated to the low frequency zonal component of wind velocity (Table 3). Taking into account the spatial structure of this mode, the correlation implies that westerlies in the Channel (winds that induce upwelling) have a stronger cooling effect to the south than the east of the island, enhancing the thermal gradient across the front of Fig. 5b. Notice, however, that this correlation occurs only at low frequency, when wind amplitude is very small. High frequency wind variability, which captures most of wind variance, is not correlated with mode 2 time coefficients.

Mode 3 time coefficients are correlated with wind stress in the high frequency band. This is encouraging because the prevailing across-Channel spatial structure of mode 3 (Fig. 5c) indicates the sea response to wind-induced upwelling. Should this correlation stand, wind stress would be ultimately responsible for the north-south displacements of the AIS.

## SUMMARY AND CONCLUSIONS

The ultimate objective of this study of the Sicilian Channel anchovy is to understand the underlying environmental factors that determine the interannual fluctuations of the resource. Two dominant hydrographic features have clear influence on the early stages of the life cycle of the Sicilian Channel anchovy: the

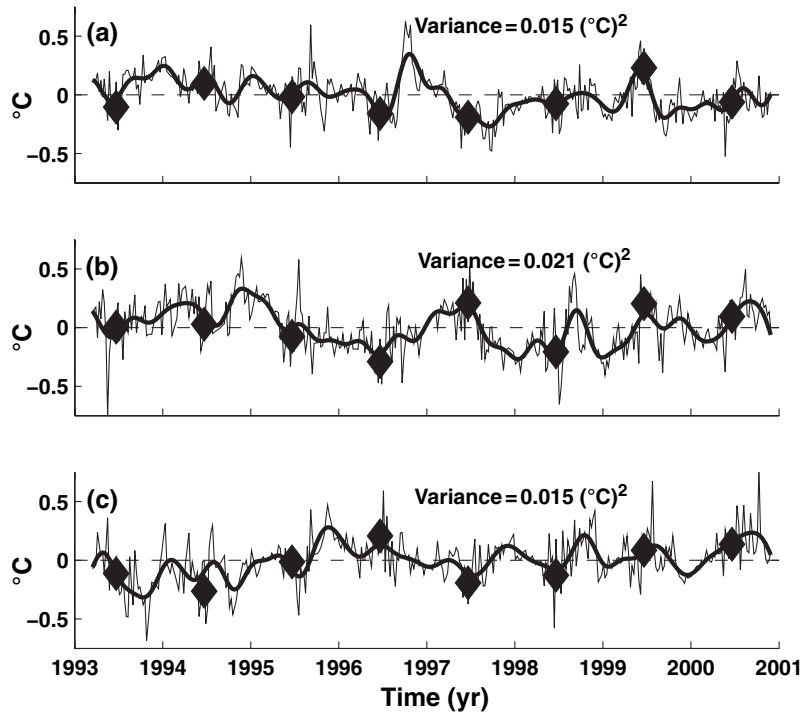


**Figure 11.** Thick line represents the time coefficients of mode 1 (a), mode 2 (b), and mode 3 (c) of the low-passed series after removing the seasonal signal estimated by eqn 6. Thin line is the sum of the low- and the high-passed (meso-scale; Fig. 8) contributions. The solid diamonds indicate the June-averaged coefficients.

alongshore AIS and the IBV and front off Cape Passero (Mazzola *et al.*, 2000; García Lafuente *et al.*, 2002; Mazzola *et al.*, 2002). The AIS path determines the temperature regime along the coast and, more importantly, in the main anchovy fishery grounds off Sciacca. Moreover, it transports the anchovy's spawning products towards the southernmost part of the island, off Cape Passero, and concentrates larvae along the front.

The SST images were decomposed into empirical modes by EOF analysis. Mode 1 contains more than twice the variance contained by modes 2 and 3 together, but these are able to modify the mean circulation pattern depicted by mode 1. Time coefficients of mode 2 manifest the seasonal weakening/enhancement of the thermal front off Cape Passero by smoothing/enhancing the thermal contrast of mode 1 spatial map in this area (Figs 5 and 9). They provide information on the time variability of the front which can have important biological consequences because the area is the nursery ground of anchovy larvae, among other species.

Mode 3 modifies the dominant spatial pattern arising from mode 1 whenever its time coefficients are significantly different from zero. The modification consists of a north (south) displacement of the stream with negative (positive) time coefficients (Fig. 10), which varies the position and extension of the coastal area flooded by the warm water of the AIS. Figure 3

indicates that when the AIS does not pass near the main fishing grounds off Sciacca, where adults concentrate, spawning there is reduced (left panels of Fig. 3), affecting the overall anchovy spawning in the Channel. The offshore displacement of the AIS would account for the low spawning of anchovy observed in 1999 and 2000 (Mazzola *et al.*, 2002). Time coefficients of mode 3 have the potential for describing such environmental conditions.

Surface circulation changes deduced from EOF analysis of SST images were compared with *in situ* hydrographic observations. The values of time coefficients of the empirical modes during 1998 to 2000 agree qualitatively well with the interpretation given above, confirming that they are potentially useful indices of hydrography.

The relationship of external forces with the empirical modes were analysed. Seasonal changes are mainly captured by the combination of modes 1 and 2, the time coefficients of mode 2 representing the seasonal enhancement of the ISFs. Interannual variability of the time coefficients of these modes produce a similar variability of the strength of the front and are correlated with the low-frequency signal of zonal wind stress over the Channel. High-passed series of the time coefficients of mode 3 are correlated with high-frequency zonal wind stress, suggesting that this mode is the footprint of the wind-induced upwelling in the Channel, a fact also suggested by the spatial map of the mode (Fig. 5c).

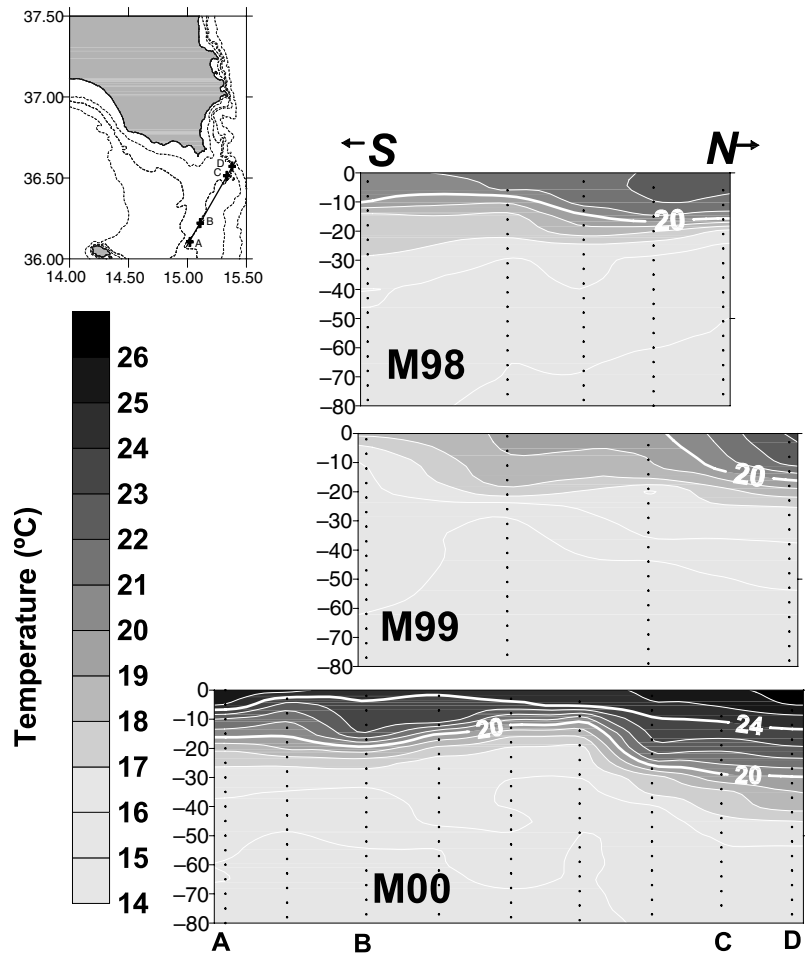


**Figure 12.** Temperature-depth sections along the line marked on the map in the upper left corner during the M98, M99 and M00 oceanographic surveys. Letters help orientate the section.

**Table 3.** Correlation between the time-coefficient series of each mode and the external meteorological forces for low- and high-frequency bands. Monthly North Atlantic Oscillation (NAO) index has been used to study only the low-frequency correlations. Absolute values above 0.393 are significant at the 99% significance level and have been shaded.

Mode	Air temperature	$U_{\text{wind}}$	$P_{\text{atm}}$	$NAO_{\text{index}}$
Low frequency band				
M1	-0.55	0.19	0.17	0.09
M2	0.23	0.50	0.37	0.36
M3	-0.11	-0.04	-0.26	-0.35
High frequency band				
M1	-0.21	0.35	-0.04	
M2	0.05	0.05	0.08	
M3	-0.29	0.46	-0.07	

Regarding anchovy's reproductive behaviour, a favourable warm temperature regime in the main fishing grounds off Sciaccia is a key factor for successful spawning. Such conditions are met by a negative

anomaly of mode 3, as in M98 when, moreover, the negative June-averaged value was accompanied by short and strong episodes of negative anomaly. These episodes are related to easterlies, thereby allowing us to infer that these winds favour spawning conditions. Positive anomalies of modes 1 and 2 indicate enhanced thermal fronts, and in turn, higher particle concentration and increased food availability. This may have a positive impact on anchovy recruitment. Table 3 indicates that cold years with predominance of low-frequency westerlies produce positive anomalies of modes 1 and 2 and, hence, favourable feeding conditions in the nursery grounds.

The suitable combination of the negative anomaly of mode 3 and positive anomaly of modes 2 and 1 would provide optimal conditions for recruitment success. Such a combination was partially met in 1997 (strong negative anomaly of mode 3, strong positive anomaly of mode 2 but negative anomaly of mode 1), which could account for the highest estimate of anchovy spawning biomass in 1998, from all the 1998–2000 DEPM surveys (Mazzola *et al.*, 2002).

## ACKNOWLEDGEMENTS

This work was conducted under the auspices of the European Union projects 'Distribution Biology and Biomass Estimates of the Sicilian Channel Anchovy' (MED96-052, MAGO1) and 'The Sicilian Channel Anchovy Fishery and the underlying Oceanographic and Biological Processes conditioning their Inter-annual Fluctuations' (MED98-070, MAGO2). We are grateful to the captain and crew of the R/V URANIA for their help in data acquisition. We are also grateful to the DFD (Deutsches Fernerkundungs Datenzentrum) for providing us with the SST images. J. Delgado acknowledges a fellowship of the University of Malaga linked to these projects. F. Criado acknowledges the fellowship AP2000-3951 of the Spanish Ministry of Education.

## REFERENCES

- Agostini, V. and Bakun, A. (2002) 'Ocean triads' in the Mediterranean Sea: physical mechanisms potentially structuring reproductive habitat suitability (with example application to European anchovy *Engraulis encrasicolus*). *Fish. Oceanogr.* **11**:129-142.
- Astraldi, M., Balopoulos, S., Candela, J. et al. (1999) The role of straits and channels in understanding the characteristics of the Mediterranean circulation. *Prog. Oceanogr.* **44**:65-108.
- Bakun, A. (1996) *Patterns in the Ocean: Ocean processes and Marine Population Dynamics*. University of California Sea Grant, San Diego, CA, USA, in co-operation with Centro de Investigaciones Biológicas de Noroeste, La Paz, Baja, California Sur, Mexico, 323 pp.
- Bakun, A. (1998) Ocean triads and radical interdecadal stock variability: bane and boon for fishery management science. In: *Reinventing Fisheries Management*. T.J. Pitcher, P.J.B. Hart & D. Pauly (eds) London: Chapman & Hall, pp. 331-358.
- Borja, A., Uriarte, A., Egana, J., Motos, L. and Valencia, V. (1998) Relationships between anchovy (*Engraulis encrasicolus*) recruitment and environment in the Bay of Biscay (1967-1996). *Fish. Oceanogr.* **7**:375-380.
- Font, J., Salat, J. and Tintoré, J. (1988) Permanent features of the circulation in the Catalán Sea. In: *Océanographie Pélagique Méditerranéenne*. H.J. Minas & P. Nival (eds) *Oceanol. Acta* **9**:51-57.
- García, A. and Palomera, I. (1996) Anchovy early life history and its relation to its surrounding environment in the Western Mediterranean basin. *Sci. Mar.* **60**:155-166.
- García Lafuente, J., García, A., Mazzola, S. et al. (2002) Hydrographic phenomena influencing early life stages of the Sicilian Channel anchovy. *Fish. Oceanogr.* **11**:31-44.
- Hotelling, H. (1933) Analysis of a complex of statistical variables with principal components. *J. Educ. Psy.* **24**:498-520.
- Hutchings, L., Barange, M., Bloomer, S.F. et al. (1998) Multiple factors affecting South African anchovy recruitment in the spawning, transport and nursery areas. In: *Benguela Dynamics. Impacts of Variability on Shelf-sea Environments and their Living Resources*. S.C. Pillar, C.L. Moloney, A.L.I. Payne & F.A. Shillington (eds) *S. Afr. J. Mar. Sci.* **19**:211-225.
- Jones, P.D., Jonsson, T. and Wheeler, D. (1997) Extension to the North Atlantic Oscillation using early instrumental pressure observations from Gibraltar and south-west Iceland. *Int. J. Climat.* **17**:1433-1450.
- Lagerloef, G.S. and Bernstein, R.L. (1988) Empirical orthogonal analysis of advanced very high resolution radiometer surface temperature patterns in the Santa Barbara Channel. *J. Geophys. Res.* **93**:6863-6873.
- Lermusiaux, P.F.J. (1999) Estimation and study of mesoscale variability in the Strait of Sicily. *Dyn. Atm. Ocean.* **29**:255-303.
- Lermusiaux, P.F.J. and Robinson, A.R. (2001) Features of dominant mesoscale variability, circulation patterns and dynamics in the Strait of Sicily. *Deep-Sea Res. I* **48**:1953-1997.
- Lloret, J., Palomera, I., Salat, J. and Sole, I. (2004) Impact of freshwater input and wind on landings of anchovy (*Engraulis encrasicolus*) and sardine (*Sardina pilchardus*) in shelf waters surrounding the Ebro River delta (north-western Mediterranean). *Fish. Oceanogr.* **13**:102-110.
- Manzella, G.M.R., Hopkins, T.S., Minnett, P.J. and Nacini, E. (1990) Atlantic water in the Strait of Sicily. *J. Geophys. Res.* **95**:1569-1575.
- Mazzola, S., Garcia, A. and Garcia Lafuente, J. (2000) Distribution, Biology and Biomass estimates of the Sicilian Channel anchovy, DG XIV, MED96-052, Final Report, 151 pp.
- Mazzola, S., Garcia, A. and Garcia Lafuente, J. (2002) The Sicilian Channel anchovy fishery and the underlying oceanographic and biological processes conditioning their inter annual fluctuations. DG XIV, MED98-070, Final Report, 268 pp.
- Onken, R. and Sellschopp, J. (1998) Seasonal variability of flow instabilities in the Strait of Sicily. *J. Geophys. Res.* **103**:24799-24820.
- Pinardi, N., Korres, G., Lascaratos, A., Roussenov, V. and Stannev, E. (1997) Numerical simulation of the interannual variability of the Mediterranean Sea upper circulation. *Geophys. Res. Lett.* **24**:425-428.
- Preisendorfer, R.W. (1988) *Principal Component Analysis in Meteorology and Oceanography*, New York: Elsevier, 425 pp.
- Quintanilla, L.F. and García, A. (2001a) Daily Egg Production for estimating the Sicilian Channel anchovy spawning biomass in 1998 and 1999. *Rapp. Comm. Int Mer Médit.* **36**:256.
- Quintanilla, L.F. and García, A. (2001b) Methodological, biological and environmental factors affecting the DEPM parameters variability in the Mediterranean anchovy. *Rapp. Comm. Int Mer Médit.* **36**:311.
- Robinson, A.R., Sellschopp, J., Warn-Varnas, A. et al. (1999) The Atlantic Ionian Stream. *J. Mar. Sys.* **20**:113-128.
- Simpson, J.J. (1994) Remote sensing in fisheries: a tool for better management in the utilization of a renewable resource. *Can. J. Fish. Aquat. Sci.* **51**:743-771.
- Sirovich, L. and Everson, R. (1992) Analysis and management of large scientific databases. *Int. J. Supercomp. Appl.* **6**:50-68.
- Vargas, J.M., García Lafuente, J., Delgado, J. and Criado, F. (2003) Seasonal and wind-induced variability of sea surface temperature patterns in the Gulf of Cádiz. *J. Mar. Sys.* **38**:205-219.
- Wang, D.C.C., Vagnucci, A.H. and Li, C.C. (1983) Digital image enhancement: a survey. *Comp. Vis. Graph. Image Process.* **24**:363-381.